Journal of South American Earth Sciences 33 (2012) 110–118

Contents lists available at ScienceDirect

Journal of South American Earth Sciences

journal homepage: www.elsevier.com/locate/jsames

Upper Cretaceous-Paleocene extensional phase in the Golfo San Jorge basin (Argentina): Growth-fault model, paleoseismicity and paleostress analysis

Nicolás Foix [a,b,*], José Matildo Paredes [a], Raúl Eduardo Giacosa [a,c]

[a] UNPSJB (Universidad Nacional de la Patagonia San Juan Bosco), Ruta Prov. No 1 S/N, Km 4 (9005), Comodoro Rivadavia, Chubut, Argentina
[b] CONICET (Consejo Nacional de Investigaciones Científicas y Técnicas), Argentina
[c] SEGEMAR (Servicio Geológico Minero Argentino) Delegación Regional Comahue, CC 228 (8332), General Roca, Río Negro, Argentina

ARTICLE INFO

Article history:
Received 29 January 2011
Accepted 24 July 2011

Keywords:
Extensional phase
Fault-growth model
Paleoseismicity
Paleostress
Late Cretaceous-Paleocene
Golfo San Jorge basin

ABSTRACT

A total of 170 synsedimentary normal faults preserved in the marine Salamanca Formation (Early Paleocene of the Golfo San Jorge basin) were described from exposures of the Northern Flank of the basin. The result of the paleostress analysis of those normal faults indicates an NE-SW (49°) extensional direction during Early Paleocene times. Synsedimentary normal faults and seismites in the unit demonstrate the occurrence of an extensional tectonic event coeval with the deposition of the Salamanca Formation.

Available 3D seismic surveys of the subsurface of the basin allowed recognizing asymmetric, fault-bounded Upper Cretaceous-Paleocene depocentres, identifying at least two main tectonic pulses in this extensional phase. The mapping of normal faults from seismic attributes (e.g. time slices) is WNW-ESE (278°–98°), a trend that apart significantly from outcrop results. The major faults in the subsurface that affect the Early Paleocene succession are the result of the extensional reactivation of Lower Cretaceous normal faults, which are mainly related to pre-existing structures in the basement of the basin. The D/L ratio of normal faults in the subsurface give smaller values than those based on theoretical relationships, being considered as sub-displaced normal faults. These low D-L values imply that the length of the major Paleocene faults was reached earlier by inheritance of previous faults. In addition, the subsurface lengths of faults allowed estimating paleoearthquake magnitudes greater to $M \approx 5$ from empirical relations, matching with previous results obtained from the analysis of soft-sediment deformational structures preserved in the Salamanca Formation. This study displays at several scales the nature, origin and tectonic products of the Upper Cretaceous-Paleocene extensional phase in the Golfo San Jorge basin.

1. Introduction

The Golfo San Jorge basin was formed in response to the break-up of the Gondwana paleocontinent during the Middle Jurassic and Early Cretaceous, following its evolution during the subsequent drift of the South American plate in the remainder of the Cretaceous and Cenozoic in a discontinuous extensional regime that lasted in the Early Miocene (Figari et al., 1999; Giacosa et al., 2004, 2006). The basin is broadly E–W oriented and located between the North Patagonian Massif and the Deseado Region, in the south Atlantic margin of Patagonia Argentina (Fig. 1A). During the evolution of the basin took place at least four extensional phases (Figari et al., 1999), where the Upper Cretaceous-Paleocene extensional phase has not described in detail so far.

Conceptually, two distinctive relationships between length and maximum displacement of normal faults have been tested in the last decades. The most widely used model suggest fault evolution by simultaneous increasing in length and maximum displacement either by growth of isolated faults or by linkage of fault segments (Walsh and Watterson, 1987, 1988; Bürgmann et al., 1994; Cowie y Scholz, 1992; Gillespie et al., 1992; Dawers et al., 1993; Schlische et al., 1996). The second genetically-based model involves an early increasing in fault-length and subsequent increasing in the displacement, and can be regarded to inheritance of a previous fault during the reactivation of normal fault systems (Walsh et al., 2002; Vétel et al., 2005; Manzocchi et al., 2006).

* Corresponding author. UNPSJB (Universidad Nacional de la Patagonia San Juan Bosco), Ruta Prov. No 1 S/N, Km 4 (9005), Comodoro Rivadavia, Chubut, Argentina. Tel.: +54 297 4550339; fax: +54 297 4559616.
E-mail address: nicofoix@unpata.edu.ar (N. Foix).

0895-9811/$ – see front matter © 2011 Elsevier Ltd. All rights reserved.
doi:10.1016/j.jsames.2011.07.005

Studies of recent earthquakes have shown that the magnitude and seismic moment can be related to the slip and dimensions of the rupture (Utsu and Seki, 1954; Kanamori and Anderson, 1975; Wyss, 1979; Singh et al., 1980; Purcaru and Berckhemer, 1982; Scholz, 1982; Wesnousky, 1986; Darragh and Bolt, 1987; Wells and Coppersmith, 1994), proposing empirical relations between earthquake magnitude and fault rupture area/length (Wells and Coppersmith, 1994) based on dimensions of seismogenic structures.

This contribution focuses on the structural characterization and tectonic evolution of normal faults during the Upper Cretaceous-Paleocene extensional phase in the Golfo San Jorge basin (Patagonia, Argentina). The tectonic analysis is based on detailed description of fault geometry, trending, D-L values and paleostress-field analysis that support from different lines of evidence and at different scales a viable fault-growth model compatible with the seismic activity recognized by Foix et al. (2006, 2008). In addition, at least two tectonic pulses in this extensional phase were recognized from a detailed interpretation of vertical seismic sections.

The goals of the paper can be summarized under three headings: 1) to analyze the Paleocene tectonic structures and to determine the principal paleostress axes, 2) to discuss the more appropriated fault-growth model for Upper Cretaceous-Paleocene normal faults, and 3) to show a linkage between the inferred fault-growth model and previously recognized evidences of paleoearthquakes.

2. Materials and methods

This study comprises the description and interpretation of normal faults in the northern part of Golfo San Jorge basin based on subsurface and outcrop data. The fieldwork consisted of the description of the geometry and kinematics of normal faults preserved in the Lower Paleocene Salamanca Formation.

Synsedimentary, mesoscopic normal faults were used to estimate P-T axes, which are not stress axes, but rather are the principal axes of the incremental strain tensor for fault movement (Marrett and Allmendinger, 1990; Marrett and Peacock, 1999). The determination of principal paleostress axes was realized through the method of Right Dihedra (Angelier and Mechler, 1977; Angelier, 1989, 1994), using measurements of fault plane–striation pairs. The Right Dihedra Method is a graphic method based on the assumption that when all faults move independently of each other within the same stress. Analyzing the Upper Cretaceous-Paleocene extensional phase in the Golfo San Jorge basin, where the deformation is dominated by pre-existing structures, the Right Dihedra method is considered more appropriate than paleostress inversion (e.g. Lopes Cardoso and Behrmann, 2006). For P-T axes calculations we employed a 2001 version of FaultKin software (Allmendinger, 2001).

The subsurface data consisted of well-logs, coherence images and cross-sections obtained from 3D seismic surveys. Vertical throws of normal faults were measured from closely spaced well-log correlations. The 3D reflection seismic information allowed us to characterize the orientation, geometry and deformation patterns of normal fault systems at a sub-regional scale.

3. Geological setting

3.1. Structural framework

Based on their tectonic features, the basin can be divided in three major regions (Figari et al., 1999): the Eastern Region (including the Northern Flank, Southern Flank and basin center), the San Bernardo Fold-Belt area and the Western Region (Fig. 1B). The Eastern Region shows an extensional style characterized by WNW-ESE normal faults with an N-S asymmetric cross-profile, the Northern Flank being steeper than the Southern Flank (Fig. 1C); major depocenters are located in the basin center area. The major normal faults dip to SW in the Northern Flank and Center of Basin, whereas in the Southern Flank most faults dip toward the NE.

The extensional regime in Patagonia began in Middle Jurassic times (Fig. 2) with a Basin and Range style (Urien, 1996), characterized by NW-SE depocenters with volcaniclastic and lacustrine

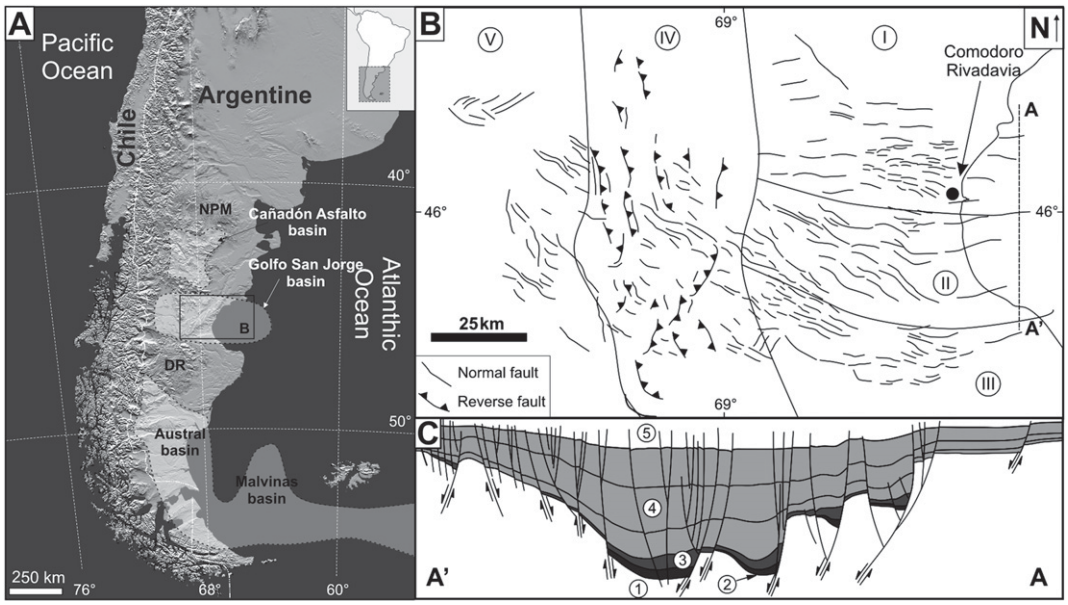

Fig. 1. (A) Radar image of the southern part of South America. Main mesozoic sedimentary basins in Patagonia (Argentina), with location of the Golfo San Jorge Basin. NPM: North Patagonian Massif. DR: Deseado Region. (B) Structural regions of the Golfo San Jorge Basin (modified from Figari et al., 1999). Key = I: Northern Flank, II: Center of Basin, III: Southern Flank, IV: San Bernardo Fold Belt and V: Western Region. (C) North-South seismic section (A–A′) showing the basin asymmetry. Key: 1) Paleozoic basement. 2) Marifil Complex (Jurassic volcanites). 3) Las Heras Group (Neocomian sedimentary rocks). 4) Chubut Group (Cretaceous sedimentary rocks). 5) Cenozoic sedimentary rocks.

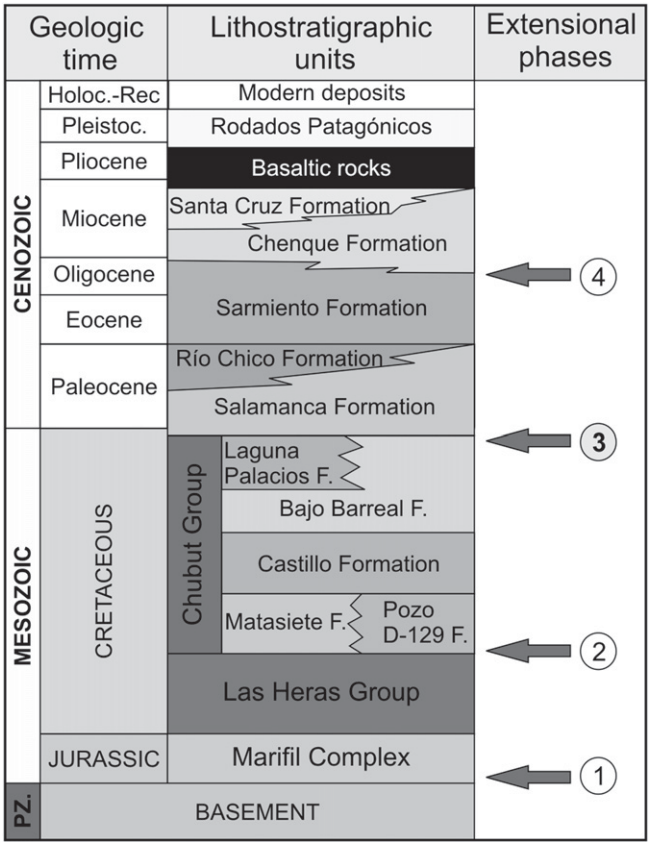

Fig. 2. Synthetic lithostratigraphy and main extensional phases in the Golfo San Jorge basin. The initial extensional phase (1) is related to the initial rifting and half-graben stage of the basin during Middle to Upper Jurassic. A second tectonic phase (2) allowed the accumulation of the Chubut Group (Cretaceous). The last two extensional phases (3, 4) occurred during the Upper Cretaceous-Paleocene and Lower Miocene respectively, favoring the development of transgressive events in the basin (modified from Figari et al., 1999).

deposits. The infill of half-grabens is represented by the Jurassic Marifil Complex (early synrift) and the Lower Cretaceous Las Heras Group (late synrift), better represented in the Western Region, and show the marginality of the Eastern Region during the rift-phase (Figari et al., 1999). A second major extensional/transtensional phase of reactivation took place in the mid-Cretaceous in the Eastern Region along WNW-ESE normal faults, providing accommodation for deposition of the "Chubutiano" or Chubut Group in lacustrine and fluvial environments (Figari et al., 1999). Tectonic control is evident in the deposits of the lacustrine Pozo D-129 Formation, the fluvial Matasiete Formation and partially on the fluvial Castillo Formation. The remainder of the Chubut Group is related to a thermal subsidence stage (Figari et al., 1999), showing gradual thickness variations at regional scale.

In the Maastrictian-Danian, an Atlantic transgression deposited the Salamanca Formation in the Eastern Region. The marine incursion has been reinforced by the extensional tectonic activity (Fig. 2), by the recognition of mesoscopic, synsedimentary normal faults (Fossa-Mancini, 1932; Urien et al., 1981; Zambrano, 1981; Chelotti, 1997; Giacosa et al., 2006) and soft-sediment deformational structures interpreted as "seismites" (Foix et al., 2006, 2008). The late extensional phase of the basin took place in the Lower Miocene during the deposition of the marine Chenque Formation (Urien et al., 1981; Figari et al., 1999; Giacosa et al., 2006). Since Middle Miocene times, the Golfo San Jorge basin has been subjected to an erosive regime related to the elevation of the Andean Ranges, to the formation of the San Bernardo Fold Belt and to an overall fall in the sea level (Legarreta et al., 1990).

During the Late Cretaceous, south of 43°30′S, the foreland area was intruded and partly covered by within-plate volcanic rocks, whereas mountain-building and arc processes in the region stopped; contemporaneously and subsequently, Palaeocene to Oligocene extensional depocentres, interfingered with volcanic activity, were developed at the foreland zone (Folguera et al., 2011; Folguera and Ramos, 2011).

3.2. Stratigraphy of the study area

The stratigraphy of the study area is characterized by a near-horizontal succession of Cenozoic sedimentary rocks onlapping a volcanic basement of Jurassic age. The Cretaceous succession is not exposed at outcrops. The older sedimentary rocks correspond to the Salamanca Formation, composed of four major sections known as "Glauconítico", "Fragmentosa", "Banco Verde" and "Banco Negro Inferior". The "Glauconítico" section is not exposed in the study area, and represents estuarine sedimentary conditions. The "Fragmentosa" section is a 100–130 m thick section of poorly consolidated, laminated or massive mudstones, attributed to inner-shelf marine environments (Legarreta et al., 1990; Legarreta and Uliana, 1994). The "Banco Verde" section is a distinctive sandstone package 8–15 m thick with abundance of glauconitic grains (Feruglio, 1949) that represent sandstone bars and channels preserved in shoreface environment. The "Banco Verde" section has been interpreted as an estuarine sandstone complex (Legarreta et al., 1990; Legarreta and Uliana, 1994) and is a distinctive

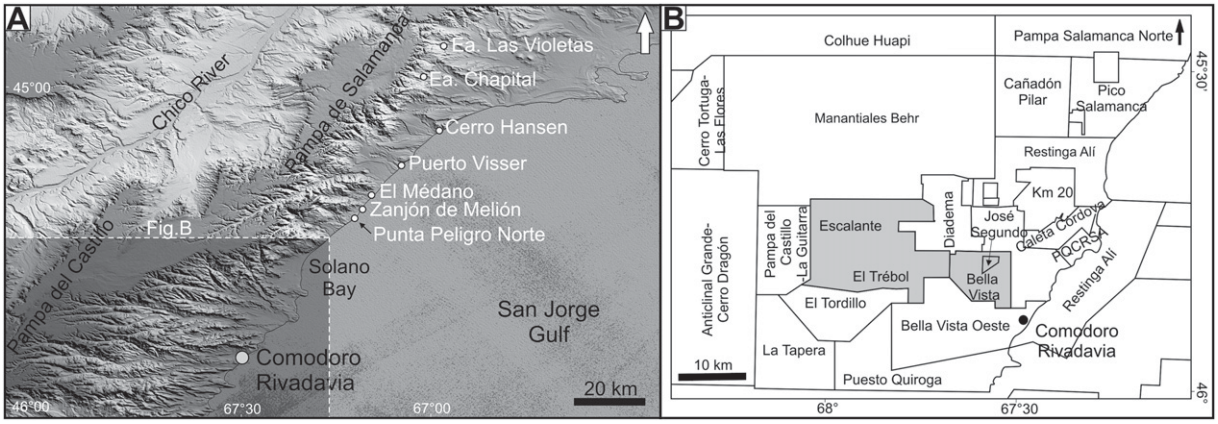

Fig. 3. (A) Digital elevation model (DEM) with location of studied localities. Structural data were obtained in the better exposures of the Salamanca Formation, northward Comodoro Rivadavia city. (B) Map of main oil fields in the Northern Flank of Golfo San Jorge basin. Subsurface data were analyzed from Escalante, El Trébol and Bella Vista oildfields.

stratigraphic marker in the subsurface of the study area. The marine–continental transition strata, known as "Banco Negro Inferior" (Feruglio, 1949) is composed of tabular, massive or horizontally-laminated black mudstones related to marsh, swamp and mangrove, poorly-drained anoxic depositional environments (Feruglio, 1949; Andreis et al., 1975; Legarreta et al., 1990; Legarreta and Uliana, 1994).

4. Results

Structural data include outcrop and subsurface information. Mesoscale normal faults were observed from exposures located northward Comodoro Rivadavia (Fig. 3A). The use of subsurface information allowed describing the structure in unexposed sectors of the Northern Flank of the basin near Comodoro Rivadavia, including Bella Vista, Escalante and El Trébol oil fields (Fig. 3B).

4.1. Outcrop data

A total of 170 synsedimentary normal faults were measured in the Fragmentosa and Banco Verde Sections (Salamanca Formation). Mesoscopic normal faults (<1 m of displacement) are the most common tectonic features and often show a domino pattern (Fig. 4A), whereas the larger faults are mostly planar or slightly listrics (Fig. 4B). Deformation in hanging-wall blocks consist of antithetic fault systems (Fig. 4B) and rollover-folds (Fig. 4C). Fault planes display slickensides and slickenlines with rare lateral component (pitch = 80–90°) (Fig. 4D).The faults show vertical decreasing in the throw, until died-out at the fault-tip (Fig. 4E), resulting in a thickening of the hanging-wall blocks with expansion index of 1.3–1.35 (Fig. 4E and F). Fault planes and fractures commonly contain 1–3 cm thick veins of gypsum, and rarely calcite infill. Dip changes in the fault planes are related to lithological changes, decreasing in less competent rocks as mudstones and increasing in consolidated sandy-strata (Fig. 4F).

The trending of normal faults shows variation in different localities (WNW-ESE, NW-SE, NNW-SSE, NNE-SSW, NE-SW), with an azimuth average of 157° (Fig. 5). Many of the faults are dipping toward the SW and dip between 30° and 90°.

The paleostress analysis from 170 mesoscopic normal faults shows an NE-SW ($\sigma 3$ = 49°) extension direction during the Early Paleocene (Salamanca Formation) (Fig. 6). T-axes show

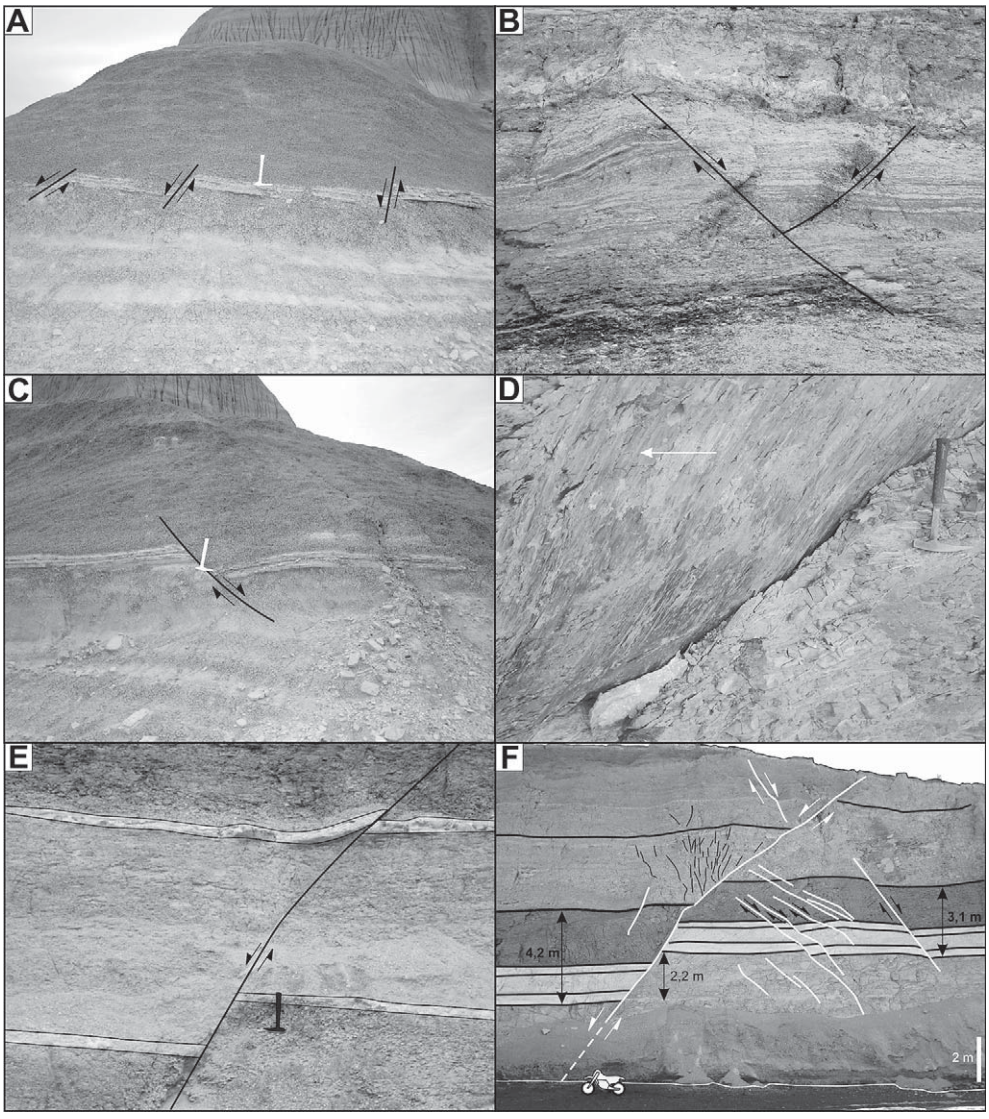

Fig. 4. Main features of the mesoscopic normal faults in the Salamanca Formation. Hammer: 0.3 m. (A) Domino pattern. (B) Slightly listric fault plane with antithetic normal fault. (C). Roll-over folds in the hanging-wall block. (D) Kinematic indicators measured on the mesoscale fault planes (arrow: slickenlines). (E) Thickening of hanging-wall blocks with expansion index of 1.3. (F) Synsedimentary normal fault (expansion index = 1.35) with changes in the dip angle due to lithological variations.

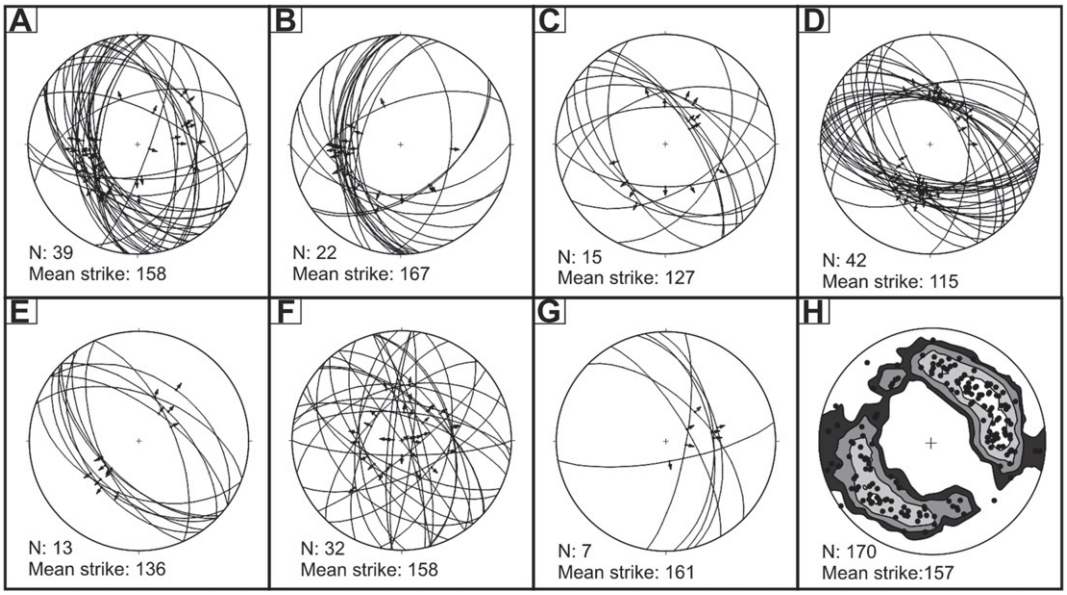

Fig. 5. Wülf stereograms with lower hemisphere projections of normal faults and striations from the studied localities. (A) Punta Peligro Norte. (B) Zanjón de Melión. (C) El Médano. D- Puerto Visser. (E) Cerro Hansen. (F) Estancia Chapital. (G) Estancia Las Violetas. (H) Contorned stereogram of 170 poles (total of faults).

a considerable dispersion reflecting differences in the extension directions for the different localities, discussed in 5.1.

4.2. Subsurface data

Normal fault systems observed using seismic attributes (e.g. time slices, coherence images) at Paleocene levels correspond to the upward propagation of basement faults that branch upward in Cenozoic levels (Fig. 7A and B). The Paleocene normal fault systems in the Northern Flank conforms wide (2–7 km) areas where numerous fault segments overlap, that in plan view can be followed by tens of kilometers (Fig.7A). The major normal fault systems are arranged in a WNW-ESE (278°–98°) direction, obtained from the orientation of 200 fault segments (Fig.7A). Most faults are dipping toward the S-SSE and individual fault-lengths range from 4 to 7 km.

Although no systematical measurements were realized, well-log correlations across the fault planes allowed recognizing changes in the vertical throws along the strike of the fault segments. Throw values of up to 72 m were obtained in the center of a major fault segment, instead toward the tip of the segment the vertical throw reduces to a few meters. The lateral relay of normal faults is defined by transfer zones, with overlaps up to 2.5 km long and oversteps ranging 0.2–1.2 km.

Vertical seismic sections show high-angle, planar or slightly listric faults with domino-style and rotated blocks (Fig.7B). The upward propagation of normal faults commonly generates monocline folds near the fault-tips, showing an upward decreasing in vertical throws. The most important structural complexity is developed in the hanging-wall blocks, with rollover-folds, grabens and synthetic or antithetic faults (Fig.7B). Locally, well defined, asymmetric, tectonic-controlled Upper Cretaceous-Paleocene seismostratigraphic intervals were recognized in the Escalante oilfield (Fig.7C and D).

5. Discussion

5.1. Paleostress analysis

Most paleostress analysis avoid information offered by inherited faults, because the distribution of orientations of reactivated weakness planes does not provide firm constrains on the orientation of the stress-field (Angelier, 1994). On the other hand, the use of mesoscopic synsedimentary faults allows estimating both age and orientation of paleostress axes.

The causes of the extensional episode occurred during the Late Cretaceous-Early Cenozoic in the Golfo San Jorge basin are unclear, but may be related to regional intraplate stress and transtensional conditions tied to differential counterclockwise rotation of South America (Fitzgerald et al., 1990). On the other hand, Folguera et al. (2011) and Folguera and Ramos (2011) interpreted that Paleocene to Oligocene extensional depocentres, interfingered with volcanic activity, were developed at the foreland zone, whereas mountain-building and arc processes in the region stopped.

The generation of accommodation space during the deposition of the Chubut Group (Cretaceous) was related to WNW-ESE and W-E normal faulting event (Fitzgerald et al., 1990; Figari et al., 1999). A similar orientation of the faults in the subsurface was observed in

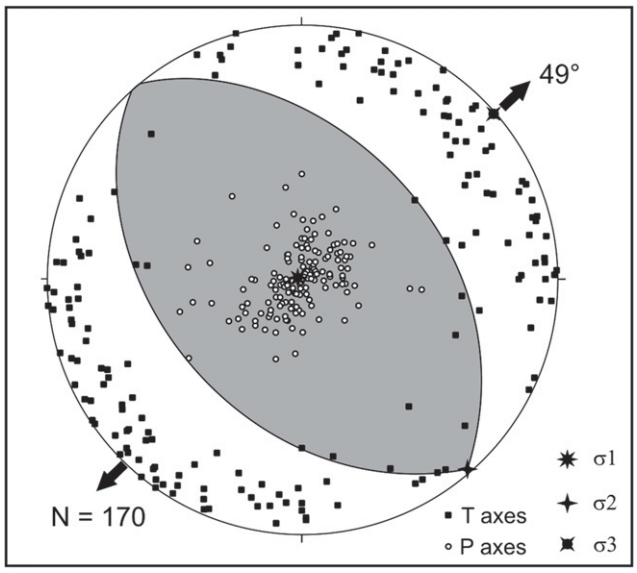

Fig. 6. Equal-area stereogram of P-T axes. NE-SW Paleocene stress-field calculated from mesoscopic normal faults affecting the Salamanca Formation.

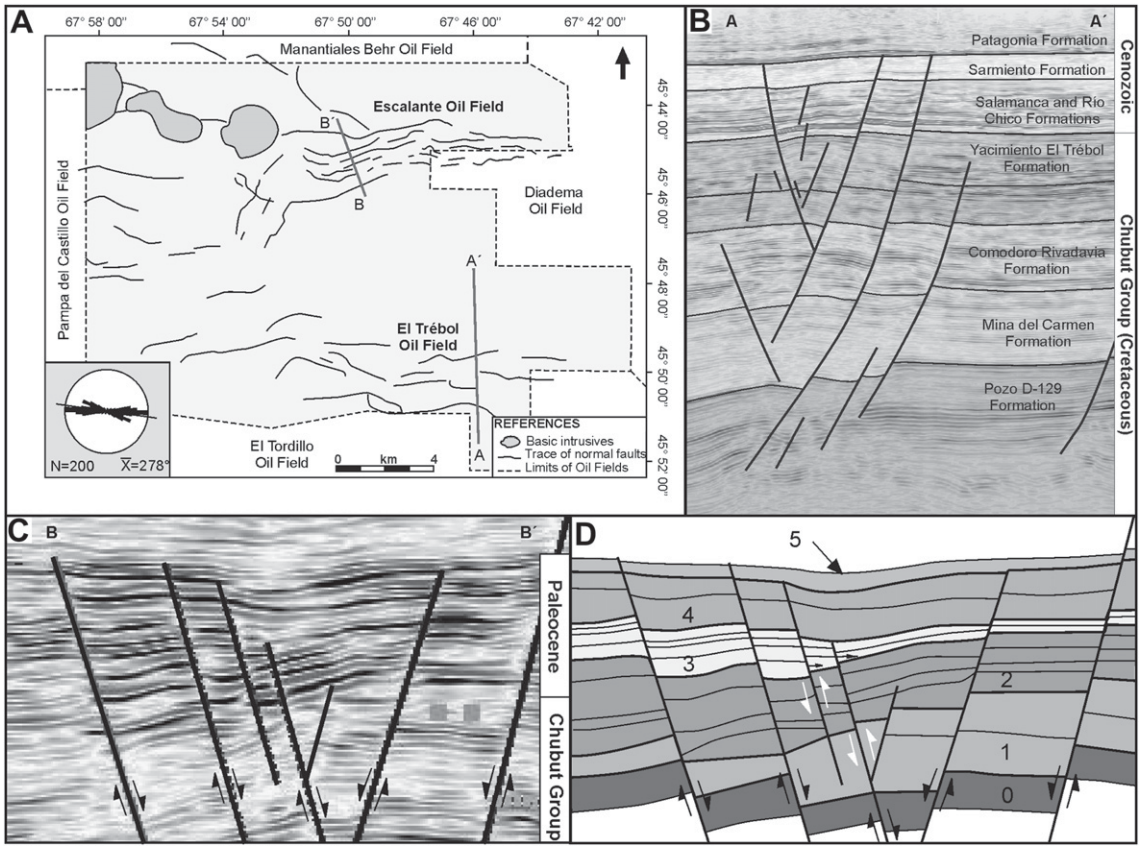

Fig. 7. (A) Interpretation of normal faults from horizontal seismic section (coherence image), Escalante and El Trébol Oil Fields. (B) Vertical seismic section of the El Trébol Fault system, displaying the extensional style. (C) Detailed vertical seismic section of the Escalante Fault system. (D) Interpretation of Fig. 7C, showing an asymmetric fault-controlled record (e.g. 1 and 3) in the Upper Cretaceous-Paleocene seismostratigraphic interval.

the study area affecting levels of the Salamanca Formation. However, the trending of mesoscopic synsedimentary normal faults at outcrops of the Salamanca Formation departs significantly from this orientation, with a mean value of 49°. The WNW-ESE orientation of large-scale faults imaged in the subsurface represents the inheritance of Cretaceous structures, but NW-SE mesoscopic normal faults obtained at outcrops can be attributed to the Lower Paleocene stress-field. The important scatter in the paleostress results (see Fig. 6) could be related to the role of pre-existing faults in modifying the orientations of principal stress axes over large areas (e.g. Zoback, 1992; Lopes Cardoso and Behrmann, 2006). Unfortunately, there is not seismic information just under the studied outcrops to check the relationship with location of reactivated faults in the subsurface. These results allow inferring a dextral oblique-slip behavior of the WNW-ESE Cretaceous normal faults under the Lower Paleocene stress-field (Fig. 8).

5.2. Tectonic control

The seismostratigraphic architecture of the Upper Cretaceous-Paleocene interval in the Escalante oilfield can be explained by a combination of half-graben geometry (Schlische, 1991; Gawthorpe et al., 1994; among others) and monocline folds originates by upward propagation of normal blind faults (Walsh and Watterson, 1987; Gawthorpe et al., 1997; Hardy and McClay, 1999; Jackson et al., 2006). A simplified reconstruction of the tectosedimentary evolution of the Escalante fault system during the Upper Cretaceous-Paleocene is shown in the Fig. 9. The first interpreted fault-controlled interval increases their thickness to the main normal fault, allowing inferring a half-graben stage (Fig. 9A). After a tabular, non-tectonically controlled interval, a new upward propagation pulse originates a monocline fold (Fig. 9B). The sedimentation related to the growing fold increases the thickness at it moves away from the fault zone, onlapping the monocline (Fig. 9C). After a new non-tectonically controlled accumulation (Fig. 9D), a post-Paleocene tectonic event affected the succession. The existence of minor reverse faults in an extensional context can be explained by upward propagation of antithetic normal faults during the evolution of monoclines (e.g. Jackson et al., 2006).

The tectostratigraphic analysis allowing infers different pulses or episodes of upward fault propagation during the Upper Cretaceous-Paleocene extensional reactivation. Probably, the temporal evolution of the Escalante Fault system responds to a relative decreasing in the upward propagation rate/supply rate ratio.

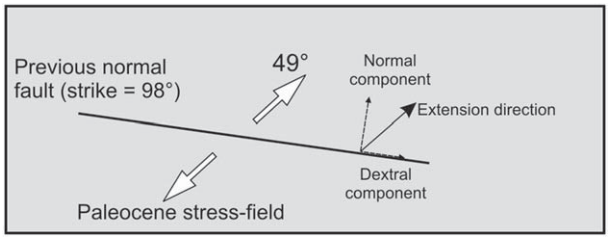

Fig. 8. Normal reactivation of WNW-ESE pre-Cenozoic normal faults would originate an oblique-extension with dextral components under the Paleocene stress-field.

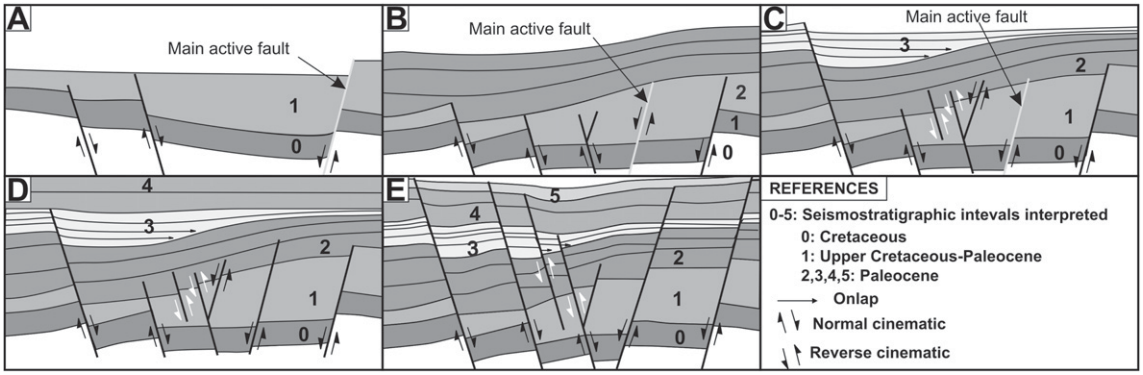

Fig. 9. Simplified tectosedimentary evolution of the Escalante fault system during the Late Cretaceous-Paleocene. (A) Tectonically-controlled deposits during the "half-graben" stage (1). (B) Deposition of tabular, not tectonically-controlled interval (2). (C) Growing of the monocline controlled the accommodation space (3). (D) Sedimentary accumulation without tectonic control (4). (E) Post-Paleocene tectonic configuration.

5.3. Paleocene fault-growth model

Most of the normal faults from outcrop and subsurface data dip to the SW in the Northern Flank of the basin. Local variations in the orientation of the normal faults can be related to disturbances in the stress-field in surroundings of major faults (Maerten et al., 2002; Lopes Cardoso and Berhmann, 2006). Upward branching of the main normal faults was observed both in seismic sections and at outcrops; the distribution of the displacement in such a large number of fault segments diminish the vertical throws of single structures.

The majority of the models used to explain the evolution of normal faults suggests simultaneous increases of length and vertical throw. Walsh et al. (2002) propose an alternative model mostly useful for reactivated faults, in which the fault-growth is accomplished by increasing cumulative displacement maintaining near constant the fault-length. In this model, the vertical throw during initial stages is lower than the displacement - length theoretical ratio (sub-displaced faults). This model with low values of displacement - length ratio explains the behavior of most of the faults reactivated during the Paleocene in the Golfo San Jorge basin. For these reasons, the upward propagation of Cretaceous normal faults during the Early Paleocene is the better growth model to explain the observed geometrical characteristics (upward decreasing in vertical throw, low Dmax/L ratios, monocline folds, small-scale reverse faults) of the extensional system in the Golfo San Jorge basin.

5.4. Paleoseismicity and fault propagation

The existence of seismically-induced liquefaction features has been related to earthquake magnitudes greater than 5 ($M > 5$) (Atkinson, 1984; Allen, 1986; Ambraseys, 1988; Enzel et al., 2000; Rodríguez-Pascua et al., 2000, 2003). The occurrence of soft-sediment deformational structures interpreted as seismically-induced deformation in strata of Salamanca and Río Chico Formations suggests similar Paleocene earthquake magnitudes (Foix et al., 2006, 2008).

Empirical relations between the earthquake magnitude and the break area/length of faults (Wells and Coppersmith, 1994) can be used to make predictions of the earthquake magnitude from the dimensions of seismogenic structures. The fault-length of Paleocene normal faults ranges from 4 to 7.5 km and, according to the relation proposed by Wells and Coppersmith (1994) these structures would generate paleoearthquakes between magnitudes 5 and 5.75 (Fig. 10).

The dimensions of the faults imaged in the subsurface are larger enough to trigger earthquakes that could develop the seismites interpreted at outcrops. The correspondence of results reinforces the hypothesis of Paleocene seismic activity with magnitudes

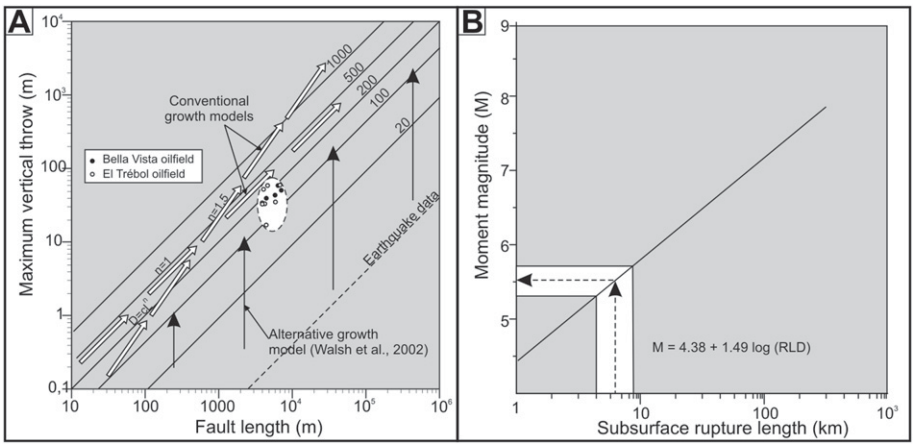

Fig. 10. (A) Maximum throw vs. fault-length log–log graphic for normal faults (modified from Walsh et al., 2002). Contours of 20, 100, 200, 500 and 1000 indicate the number of earthquakes (N) required moving cumulative fault displacements along vertical growth trends from the earthquake line. The plot of large-scale Paleocene normal faults (subsurface data) displays a wide range of vertical throws for similar fault-lengths, with low values of displacement - length ratio (sub-displaced faults). (B) Earthquake magnitudes estimated from the subsurface rupture length (RLD) using the relationship proposed by Wells and Coppersmith (1994). Individual fault segments among 5–10 km in length would produce earthquake magnitudes between 5 and 5.75.

$M > 5$. Additionally, assuming the validity of the model proposed by Walsh et al. (2002) for the growth of the Paleocene normal faults in the Golfo San Jorge basin, and considering the empirical relation between break area/length of fault proposed by Wells and Coppersmith (1994), the inheritance of fault planes dimensions (area and length of break) contributed to the generation of earthquakes of important magnitude during the Paleocene extensional reactivation.

6. Conclusions

- Paleostress analysis from mesoscopic normal faults shows an NE-SW (49°) extension direction during the Early Paleocene in the Northern Flank of the basin. The WNE-ESE orientation of large-scale Paleocene normal faults represents the inheritance of Cretaceous structures.
- The upward propagation of Cretaceous normal faults is the better fault-growth model to explain the geometric characteristics of the Paleocene faults (low values of displacement – length ratios, upward decreasing of the vertical throw, monocline folds and minor reverse faults).
- The Upper Cretaceous-Paleocene extensional phase included several tectonic pulses or events, with upward decreasing intensity.
- The WNW-ESE large-scale normal faults in the subsurface of the basin would have behaved with dextral oblique components under the Paleocene stress-field.
- The fault-length of Paleocene normal faults would be enough to generate earthquakes with magnitudes $M > 5$ (5–5.75), matching with previous estimations from soft-sediment deformational structures.

Acknowledgments

This paper is based on part of the unpublished Ph.D. thesis of the former author (Universidad Nacional de la Patagonia San Juan Bosco). The study was supported by a Ph.D. grant to the first author from the CONICET (Consejo Nacional de Investigaciones Científicas y Técnicas). The authors wish to acknowledge YPF S.A. for access to proprietary 3-D seismic reflection data and well-log data. The authors also wish to thank Carlos Costa (Universidad Nacional de San Luis) for his contribution on early drafts of this paper. The Departamento de Geología of the UNPSJB is gratefully acknowledged for logistic support during fieldwork. We thank the constructive and useful reviews of F. Bechis and an anonymous reviewer.

References

Allen, J.R.L., 1986. Earthquake magnitude-frequency, epicentral distance and soft-sediment deformation in sedimentary basins. Sedimentary Geology 46, 67–75.
Allmendinger, R.W., 2001. FaultKinWin, Version 1.1. A Program for Analyzing Fault Slip Data for Windows™ Computers.
Ambraseys, N.N., 1988. Engineering seismology: earthquake engineering and structural dynamics. Journal of the International Association of Earthquake Engineering 17, 1–105.
Andreis, R.R., Mazzoni, M., Spaletti, L.A., 1975. Estudio estratigráfico y paleoambiental de las sedimentitas terciarias entre Pico Salamanca y Bahía Bustamante, Provincia del Chubut, República Argentina. Revista Asociación Geológica Argentina 30 (1), 85–103. Buenos Aires.
Angelier, J., 1989. From orientation to magnitudes in paleostress determinations using fault slip data. Journal of Structural Geology 11, 37–50.
Angelier, J., 1994. Fault analysis and paleostress reconstruction. In: Hancock, P.L. (Ed.), Continental Deformation. Pergamon Press, New York, pp. 53–100.
Angelier, J., Mechler, P., 1977. Sur une méthode graphique de recherche des contraintes principales également utilisable en tectonique et séismologie: la méthode des diedres droits. Bulletin Societé Géologique de France 19 (6), 1301–1318.
Atkinson, G., 1984. Simple computation of liquefaction probability for seismic hazard applications. Earthquake Spectra 1, 107–123.
Bürgmann, R., Pollard, D.D., Martel, S.J., 1994. Slip distributions on faults: effects of stress gradients, inelastic deformation, heterogeneous host-rock stiffness, and fault interaction. Journal of Structural Geology 16, 1675–1690.
Chelotti, L., 1997. Evolución tectónica de la Cuenca del Golfo San Jorge en el Cretácico y Terciario: algunas observaciones desde la interpretación sísmica. Boletín de Informaciones Petroleras 49, 62–82.
Cowie, P.A., Scholz, C.H., 1992. Physical explanation for displacement-length relationship for faults using post-yield fracture mechanics model. Journal of Structural Geology 14, 1133–1148.
Darragh, R.B., Bolt, B.A., 1987. A comment on the statistical regression relation between earthquake magnitude and fault rupture length. Bulletin of Seismological Society of America 77, 1479–1484.
Dawers, N.H., Anders, M.H., Scholz, C.H., 1993. Growth of normal faults: displacement–length scaling. Geology 21, 1107–1110.
Enzel, Y., Kadan, G., Eyal, Y., 2000. Holocene earthquakes inferred from a fan-delta sequence in the Dead Sea Graben. Quaternary Research 53, 34–48.
Feruglio, E., 1949. Descripción Geológica de la Patagonia. Yacimientos Petrolíferos Fiscales 1, 1–334. Buenos Aires.
Figari, E., Strelkov, E., Laffife, G., Cid de la Paz, M., Courtade, S., Celaya, J., Vottero, A., Lafourcade, S., Martinez, R.Y Villar, H., 1999. Los sistemas petroleros de la Cuenca del Golfo San Jorge: Síntesis estructural, estratigráfica y geoquímica. 4° Congreso de Exploración y Desarrollo de Hidrocarburos, Actas, Buenos Aires, pp. 197–237.
Fitzgerald, M.G., Mitchum, R.M., Uliana, M.A., Biddle, K.T., 1990. Evolution of the San Jorge basin, Argentina. American Association of Petroleum Geologists Bulletin 74 (6), 879–920. Tulsa.
Foix, N., Paredes, J.M., Giacosa, R.E., 2006. Soft-sediment deformation structures interpreted as seismites: an example from Salamanca and Río Chico Formations, Paleocene of Golfo San Jorge Basin, Argentina. IV Latinamerican Congress of Sedimentology y XI Reunión Argentina de Sedimentología. Resúmenes, 98. San Carlos de Bariloche.
Foix, N., Paredes, J.M., Giacosa, R.E., 2008. Paleo-earthquakes in passive margin settings, an example from the Paleocene of the Golfo San Jorge basin, Argentina. Sedimentary Geology 205, 67–75.
Folguera, A., Ramos, V.A., 2011. Repeated eastward shifts of arc magmatismin the Southern Andes: a revision to the long-term pattern of Andean uplift and magmatism. Journal of South American Earth Sciences. doi:10.1016/j.jsames.2011.04.003.
Folguera, A., Orts, D., Spagnuolo, M., Rojas Vera, E., Litvak, V., Sagripanti, L., Ramos, M.E., Ramos, V.A., 2011. A review of late Cretaceous to quaternary palaeogeography of the southern Andes. Biological Journal of the Linnean Society 103, 250–268.
Fossa-Mancini, E., 1932. Faults in Comodoro Rivadavia oil field, Argentina. American Association of Petroleoum Geologist Bulletin 16 (6), 556–576. Tulsa.
Gawthorpe, R.L., Sharp, I., Underhill, J.R., Gupta, S., 1997. Linked sequence stratigraphic and structural evolution of propagating normal faults. Geology 25, 795–798.
Gawthorpe, R.L., Fraser, A.J., Collier, R.E.Ll, 1994. Sequence stratigraphy in active extensional basins: implications for the interpretation of ancient basin fills. Marine and Petroleum Geology 11, 642–658.
Giacosa, R., Foix, N., Paredes, J., Allard, J., 2006. Fallas normales e ingresiones en el Terciario marino de la Cuenca del Golfo San Jorge. 13° Reunión de Tectónica, Resúmenes, pp. 25, San Luis.
Giacosa, R.E., Paredes, J.M., Nillni, A., Ledesma, M., Colombo, F., 2004. Fallas normales de alto ángulo en el Neógeno del margen Atlántico de la Cuenca del Golfo San Jorge (46° S – 67° 30' O, Patagonia Argentina). Boletín Geológico Minero 115 (3), 537–550.
Gillespie, P.A., Walsh, J.J., Watterson, J., 1992. Limitations of dimension and displacement data from single faults and the consequences for data analysis and interpretation. Journal of Structural Geology 14, 1157–1172.
Hardy, S., McClay, K., 1999. Kinematic modelling of extensional fault-propagation folding. Journal of Structural Geology 21, 695–702.
Jackson, C.A.L., Gawthorpe, R.L., Sharp, I.R., 2006. Style and sequence of deformation during extensional fault-propagation folding: examples from the Hammam Faraun and El-Qaa fault blocks, Suez Rift, Egypt. Journal of Structural Geology 28, 519–535.
Kanamori, H., Anderson, D.L., 1975. Theoretical basis of some empirical relations in seismology. Bulletin of Seismological Society of America 65, 1073–1096.
Legarreta, L., Uliana, M.A., 1994. Asociaciones de fósiles y hiatos en el Supracretácico-Neógeno de la Patagonia: Una perspectiva estratigráfico-secuencial. Ameghiniana. Revista de la Asociación Paleontológica Argentina 31 (3), 257–281. Buenos Aires.
Legarreta, L., Uliana, M., Torres, M., 1990. Secuencias deposicionales cenozoicas de Patagonia Central: sus relaciones con las asociaciones de mamíferos terrestres y episodios marinos epicontinentales. 3° Simposio del Terciario de Chile. Actas, Concepción, pp. 135–176.
Lopes Cardoso, G.G.O., Behrmann, J.H., 2006. Kinematic analysis of the Upper Rhine Graben boundary fault system. Journal of Structural Geology 28, 1028–1039.
Maerten, L., Gillespie, P., Pollard, D.D., 2002. Effects of local stress perturbation on secondary fault development. Journal of Structural Geology 24, 153–154.
Manzocchi, T., Walsh, J.J., Nicol, A., 2006. Displacement accumulation from earthquakes on isolated normal faults. Journal of Structural Geology 28, 1685–1693.
Marrett, R., Allmendinger, R.W., 1990. Kinematic analysis of fault-slip data. Journal of Structural Geology 12 (8), 973–986.

Marrett, R., Peacock, D.C.P., 1999. Strain and stress. Journal of Structural Geology 21, 1057–1063.
Purcaru, G., Berckhemer, H., 1982. Quantitative relations of seismic source parameters and a classification of earthquakes. In: Duda, S.J., Aki, K. (Eds.), Quantification of Earthquakes. Tectonophysics, 84, pp. 57–128.
Rodríguez-Pascua, M.A., Calvo, J.P., De Vicente, G., Gómez-Gras, D., 2000. Soft-sediment deformation structures interpreted as seismites in lacustrine sediments of the Prebetic Zone, SE Spain, and their potential use as indicators of earthquake magnitudes during the Late Miocene. Sedimentary Geology 135, 117–135.
Rodríguez-Pascua, M.A., De Vicente, G., Calvo, J.P., Pérez-López, R., 2003. Similarities between recent seismic activity and paleoseismites during the late Miocene in the external Betic Chain (Spain): relationship by 'b' value and the fractal dimension. Journal of Structural Geology 25, 749–763.
Schlische, R.W., 1991. Half-graben basin filling models: new constraints on continental extensional basin development. Basin Research 3, 123–141.
Schlische, R.W., Young, S.S., Ackermann, R.V., Gupta, A., 1996. Geometry and scaling relations of a population of very small rift-related normal faults. Geology 24, 683–686.
Scholz, C.H., 1982. Scaling laws for large earthquakes: consequences for physical models. Bulletin of Seismological Society of America 72, 1–14.
Singh, S.K., Bazan, E., Esteva, L., 1980. Expected earthquake magnitude from a fault. Bulletin of Seismological Society of America 70, 903–914.
Urien, C.M., Zambrano, J.J., Martins, L.R., 1981. The basins of southeastern South America (Southern Brazil, Uruguay and eastern Argentina) including the Malvinas Plateau and suthern atlantic paleogeographic evolution. En Cuencas Sed. del Jurásico y Cretácico de América del Sur. In: Volkheimer, W.Y., Musacchio, E.A. (Eds.), Contribución del comité sudamericano del jurásico y cretácico al II Congreso Latinoamericano de Paleontología, vol. 1, pp. 45–125.
Urien, C., 1996. Las cuencas del margen continental argentino. Boletín de Informaciones Petroleras. Tercera Época 46, 80–84.
Utsu, T., Seki, A., 1954. A relation between the area of aftershock region and the energy of main-shock. Journal of Seismological Society of Japan 7, 233–240.
Vétel, W., Le Gall, B., Walsh, J.J., 2005. Geometry and growth of an inner rift fault pattern: the Kino Sogo fault Belt, Turkana rift (North Kenya). Journal of Structural Geology 27, 2204–2222.
Walsh, J.J., Nicol, A., Childs, C., 2002. An alternative model for the growth of faults. Journal of Structural Geology 24, 1669–1675.
Walsh, J.J., Watterson, J., 1987. Distributions of cumulative displacement and seismic slip on a single normal fault surface. Journal of Structural Geology 9, 1039–1046.
Walsh, J.J., Watterson, J., 1988. Analysis of the relationship between the displacements and dimensions of faults. Journal of Structural Geology 10, 239–247.
Wells, D.L., Coppersmith, K.J., 1994. New empirical relationships among magnitude, rupture length, rupture width, rupture area, and surface displacement. Bulletin of the Seismological Society of America 84, 974–1002.
Wesnousky, S.G., 1986. Earthquakes, quaternary faults, and seismic hazards in California. Journal of Geophysical Research 91, 12587–12631.
Wyss, M., 1979. Estimating maximum expectable magnitude of earthquakes from fault dimensions. Geology 7, 336–340.
Zambrano, J.J., 1981. Distribución y evolución de las cuencas sedimentarias en el continente sudamericano durante el jurásico y cretácico. En Cuencas Sede. del Jurásico y Cretácico de América del Sur. In: Volkheimer, W.Y., Musacchio, E.A. (Eds.), Contribución del comité sudamericano del jurásico y cretácico al II Congreso Latinoamericano de Paleontología, vol. 1, pp. 9–44.
Zoback, M.L., 1992. First- and second-order patterns of stress in the lithosphere: the world stress map project. Journal of Geophysical Research 97, 11703–11711.